bioRxiv preprint doi: https://doi.org/10.1101/2020.07.22.215251; this version posted July 24, 2020. The copyright holder for this preprint (which was not certified by peer review) is the author/funder. All rights reserved. No reuse allowed without permission.

Real-time colorimetric LAMP methodology for quantitative nucleic acids detection at the point-of-care

George Papadakis[1,*], Alexandros K. Pantazis[1,#], Nikolaos Fikas[1,2], Stella Chatziioannidou[1,2], Kleita Michaelidou[3], Vasiliki Pogka[5], Maria Megariti[1], Maria Vardaki[1], Konstantinos Giarentis[2], Judith Heaney[6,7], Eleni Nastouli[6,7], Timokratis Karamitros[5], Andreas Mentis[5], Sofia Agelaki[3,4], Electra Gizeli[1,2,*]

[1] Institute of Molecular Biology and Biotechnology, Foundation for Research and Technology-Hellas,100 N. Plastira Str., Heraklion 70013, Greece
[2] Department of Biology, University of Crete, Voutes, Heraklion 70013, Greece
[3] Laboratory of Translational Oncology, School of Medicine, University of Crete, Heraklion, 71110, Greece
[4]Department of Medical Oncology, University General Hospital, Heraklion, 71110, Greece
[5] National SARS-CoV-2 Reference Laboratory, Hellenic Pasteur Institute, 127 Vas. Sofias Ave., Athens 11521, Greece
[6] Advanced Pathogens Diagnostics Unit, University College London Hospitals NHS Trust, London WC1H 9AX
[7] UCL Great Ormond Street Institute of Child Health

*Corresponding authors: gpapadak@imbb.forth.gr; gizeli@imbb.forth.gr

[#] Current address: Institute of Electronic Structure and Laser, FORTH, 100 N. Plastira Str., Heraklion 70013, Greece

Abstract

Most methods applied to nucleic acids' detection at the point-of-care require either expensive and mostly bench-top instruments or simpler inexpensive systems providing qualitative results. Truly decentralized approaches to reliable, quantitative and affordable diagnostics are still missing. Here, we report the development of real-time quantitative colorimetric LAMP based on a portable and cost-effective device, the use of which requires minimal training. Main advantages of the method are the rapid analysis time (<30min); quantification over a large dynamic range (9 log units); ability to work with crude samples (saliva, tissue); demonstrated low detection limit (1-10 copies); smartphone-operation and fast prototyping (3D-printing). The system's broad detection capability is demonstrated during infectious diseases-testing for COVID-19 and pharmacogenetics for *BRAF* V600E mutation testing. Validation studies showed 97.4% and 100% agreement with qRT-PCR for SARS-CoV-2 RNA detection extracted from positive and negative patients' samples (89), respectively; and 100% agreement with ddPCR and Sanger sequencing for *BRAF* V600E mutation detection from 12 clinical biopsy samples. The new methodology provides a needed solution for affordable healthcare at the point-of-care, with emphasis on global diagnostics.

bioRxiv preprint doi: https://doi.org/10.1101/2020.07.22.215251; this version posted July 24, 2020. The copyright holder for this preprint (which was not certified by peer review) is the author/funder. All rights reserved. No reuse allowed without permission.

Over the past three decades, the invention of real-time quantitative PCR (qPCR) has brought a fundamental transformation in the field of molecular diagnostics[1-3]. Until today, the power of qPCR lies in the ability to quantify nucleic acids over an extraordinarily wide dynamic range and without the need for post-amplification manipulations[4]. However, qPCR is still a relatively complex, lab-based technology requiring thermal blocks with precise temperature control for amplification, expensive optical components for detection and sophisticated design of fluorescent probes for efficient DNA targeting or extensive optimization when using DNA dyes[5, 6]. The development of alternative methodologies for operation outside the lab and at the point-of-care (POC) in order to shorten lengthy procedures and provide fast results at a fraction of the cost is a desirable, yet, challenging task.

Loop-mediated isothermal amplification (LAMP) stands out as a simpler yet powerful alternative to PCR of exceptional specificity in the case of sequence-specific amplification since it employs 4 to 6 primers which recognize 6 to 8 different regions in the target sequence[7]. LAMP can be performed at a constant temperature (60-65°C) eliminating the need for thermal cycling[8, 9], is faster [10, 11] and less affected by inhibitors commonly present in biological samples[12, 13]. LAMP amplification can be monitored in real-time primarily through fluorescence or turbidimetry providing quantitative information[14-16]. The latter is important not only for lab-based but also for point-of-care applications as, for example, in the case of HIV viral load monitoring in resource-limited areas[14, 17]. However, the bulky and not so sensitive turbidimeters[18, 19] and expensive real-time fluorescence-machines are not ideal for POC diagnostics. The same applies to the use of sophisticated but costly microfluidic chips[20, 21] often used for real time monitoring in combination with optical[22], electrochemical[23], smartphone[24-26], acoustic[27] or other microdevices[22, 28, 29]. Moreover, fluorescent LAMP suffers similarly to PCR from high background and often inhibition of the reaction due to the increased dye concentration[30].

As an alternative, researchers have been developing assays based on naked-eye observation[26, 31] with end-point colorimetric LAMP being the most popular assay[32-37]. The above can employ simple means of heating e.g., a water bath, a thermos etc. or portable and/or battery operated instruments for isothermal amplification and eye-observation, all suitable for applications in resource-limited areas[34, 38]. Downsides of the naked-eye detection are the need of a “trained eye” for results interpretation, especially at low numbers of the target and the qualitative nature of the results[26]. Attempts to overcome the above problem include the use of digital image analysis employed in microfluidic chips with nanoliter volumes for end-point color quantification[39], a sophisticated but rather complex method. In another work, a photonic crystals-setup was employed to achieve naked-eye quantification of LAMP reactions after several rinsing and drying steps and exposure of LAMP amplicons to the surrounding space[40]. Finally, LAMP products combined with a lateral flow dipstick have been used for highly specific and visual detection of amplicons at the POC[26]. The paper-based strips are competitive end-point LAMP candidates for POC since they do not require any instrumentation; however, they are also qualitative and prone to contamination[26]. As concluded in a recent review[7], while open fluorescence-based platforms are already commercially available and can be implemented for lab-based LAMP detection, tailored-made devices’ adaptation to operational environments is still missing.

In this work, we report the design and construction of a portable biomedical device for performing real-time quantitative colorimetric LAMP (qcLAMP) at the POC. A schematic of the

bioRxiv preprint doi: https://doi.org/10.1101/2020.07.22.215251; this version posted July 24, 2020. The copyright holder for this preprint (which was not certified by peer review) is the author/funder. All rights reserved. No reuse allowed without permission.

qcLAMP device and concept is presented in Fig. 1a. The device is constructed using miniaturized electronic components produced by three-dimensional (3D) additive manufacturing and operates via an in-house developed smartphone application. For monitoring the color change during DNA amplification, a novel way of heating was introduced allowing efficient amplification with parallel visualization of the reaction by a mini digital camera controlled by a Raspberry Pi. The above, when combined with an application for digital image analysis, can extract rapidly quantitative information at a wide dynamic range of the genetic target. For the proof-of-concept, we used the qcLAMP device for the detection of SARS-CoV-2 RNA extracted from patients' samples and the *BRAF* V600E mutation using genomic DNA from formalin-fixed paraffin-embedded (FFPE) specimens. Our results prove both the suitability of the newly reported real-time qcLAMP as a reliable and versatile method for genetic testing as well as the device high technology readiness level allowing immediate implementation at the point-of-need.

Results

Device design and construction. The real-time colorimetric device was fabricated using additive manufacturing. Following the design of the device main housing unit, digital manufacturing based on 3D-printing was employed. Within this unit, all the required electronic components and an 8-slot tube-holder accommodating standard 0.2 ml Eppendorf tubes were positioned according to a CAD design; moreover, a top cover was used to apply pressure on the tubes and simultaneously provide an isolated chamber from the environment while real-time colorimetric LAMP detection takes place (Fig. 1b and c). The electronic components consist of a main electronic board, a Raspberry Pi Zero, a Raspberry Zero camera and a temperature sensor connected to a PCB resistive microheater. When the top part is positioned in place for operation, the mini camera is aligned opposite the tubes while two led lights are placed on both sides to provide stable lighting conditions in the chamber (Fig. 1d). The heating element is in direct contact only with the bottom of the tubes (~2 mm diameter of contact surface), while application of appropriate pressure (~2 MPa) from the top cover maintains good contact with the heating element. This particular setup allows for the direct inspection of the reaction progress through the side of the tube-walls combined with efficient and timely heating of the solution. The tube holder and cover top parts are held in place with the aid of magnets, which facilitate the opening and closing of the device and eliminate the need of screws. Additionally, the magnets minimize any potential variation in the applied pressure among different runs of the device.

The dimensions (11x10x10 cm) and weight (370 g) of the device are ideal for use at the POC (Fig. 1e). The housing unit is made mostly of polylactic acid (PLA) plastic and requires ~10 hours of continuous printing while the assembly of all the components can be completed in 20 min. The simple construction requirements allow for the production of several prototypes in less than a week (Fig. 1f). The device connects via Bluetooth to a smartphone or tablet and operates through an in-house developed Android application (Fig. S1).

bioRxiv preprint doi: https://doi.org/10.1101/2020.07.22.215251; this version posted July 24, 2020. The copyright holder for this preprint (which was not certified by peer review) is the author/funder. All rights reserved. No reuse allowed without permission.

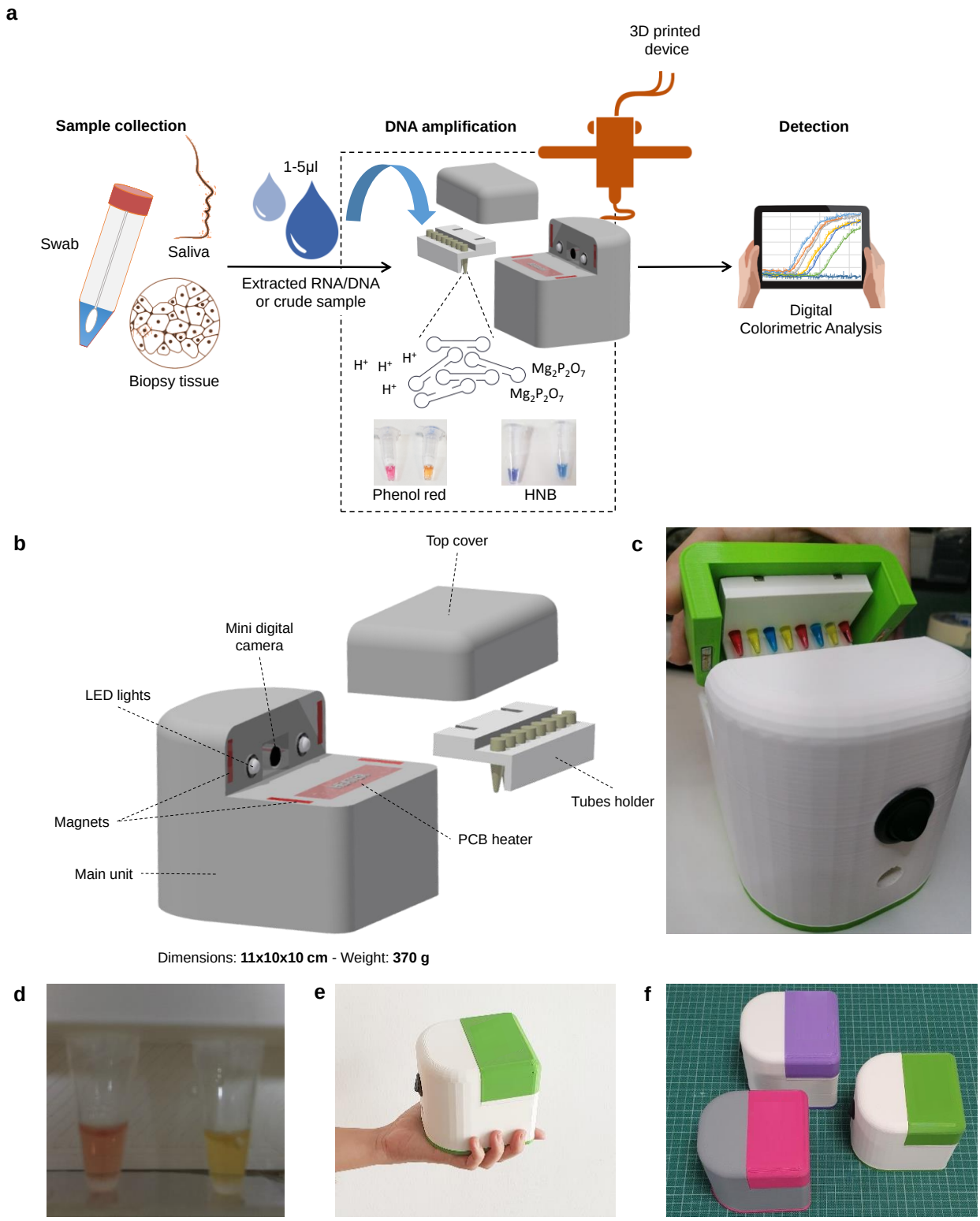

Figure 1: (a) Overview of the real-time quantitative colorimetric LAMP concept. Bottom: (b) Schematic representation of the qcLAMP device and components. (c) Photograph of the device and tubes-holder. (d) Captured image of two Eppendorf tubes inside the chamber and during operation of the device. (e) Image of the handheld device for performing qcLAMP. (f) Three prototype devices of various colors.

bioRxiv preprint doi: https://doi.org/10.1101/2020.07.22.215251; this version posted July 24, 2020. The copyright holder for this preprint (which was not certified by peer review) is the author/funder. All rights reserved. No reuse allowed without permission.

Digital image analysis. Colorimetric LAMP detection typically relies on the naked-eye evaluation of color change which is achieved through the use of different indicators such as pH[41], metal binding[42] or DNA binding[43] dyes. Since color change can often be difficult to discern under variable conditions (lighting, target concentration, etc.), smartphone cameras combined with algorithms or radiometric imaging have been proposed as a generic solution for more accurate and quantitative end-point colorimetric test –results[39, 43-46].

Here, a mini digital camera is employed for monitoring in real-time the transition through various color shades during colorimetric LAMP amplification. The camera collects non-calibrated images at predefined time intervals (6 sec minimum interval) and automatically extracts the red, green and blue (RGB) pixel values. A real-time curve is displayed plotting the difference between green and blue or green and red pixels, depending on the indicator dye. The selection of these two formulas was derived after systematic analysis of a series of images containing either the phenol red or the hydroxy napthol blue (HNB) dyes (Fig. S2a-e). When the phenol red indicator was used, the Green-Blue pixel formula responded well into discriminating the positive from the negative sample; with the HNB indicator, the Green-Red formula resulted in better discrimination.

Based on the above, the qcLAMP device was programmed so that the end-user could select any of the two formulas. The formulas are displayed in the Y-axis of a real-time plot as color index units (pixels). Figures 2a and 2b show examples of real time colorimetric LAMP reactions performed in the device at the phenol red and the HNB channels, respectively. Whole bacteria cells were used as template for the positive reactions which were run in parallel with negative control reactions without template. Regardless of the dye used in each reaction, the change in the slope of the line corresponding to the positive sample at a specific time point (14.1 and 13.3 min for the phenol red and HNB, respectively) indicates the presence of the target, as opposed to the line corresponding to the negative sample which remains almost flat throughout the monitoring period.

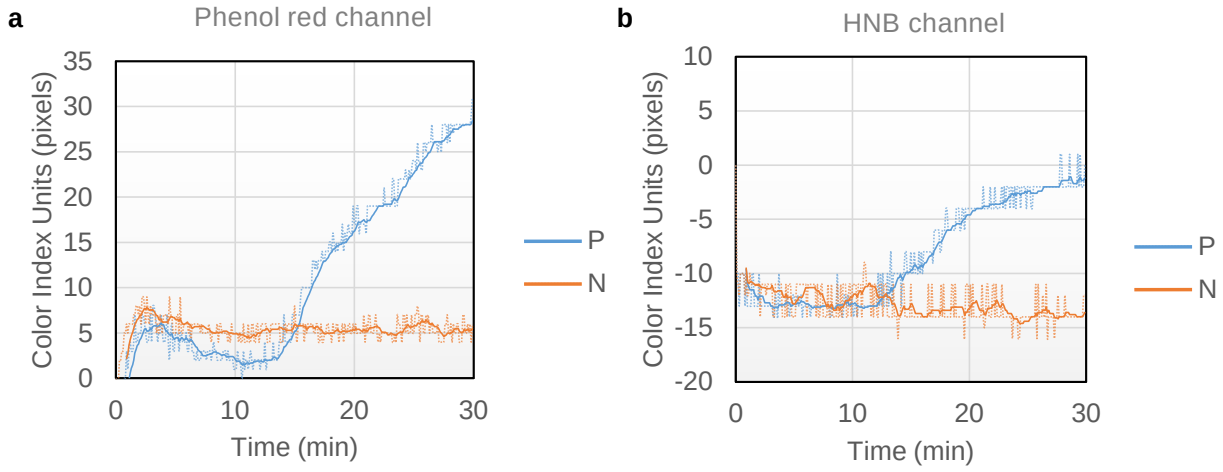

Figure 2: (a) Real-time colorimetric LAMP reactions performed inside the device using the phenol red indicator. The positive reaction (blue line) contained 10 lysed bacteria as template while the negative control contained no bacteria (orange line). (b) Similar reactions to (a), this time performed with the HNB indicator. In both cases, the heating process

bioRxiv preprint doi: https://doi.org/10.1101/2020.07.22.215251; this version posted July 24, 2020. The copyright holder for this preprint (which was not certified by peer review) is the author/funder. All rights reserved. No reuse allowed without permission.

started at t=0 min and the heater reached the required temperature (63ºC) after approximately 2 min. All reactions were stopped after 30 minutes.

Performance evaluation. For the performance evaluation of the qcLAMP, the mechanical robustness of the device was investigated as well as the speed, efficiency and sensitivity during LAMP amplification of a genetic target (*Salmonella* InvA gene). Regarding the former, potential variations in the measurements introduced by the position of the tube inside the holder were tested. Results showed excellent reproducibility in terms of the average time at which the color index slope starts to increase, i.e., a 24 sec deviation (15.7±0.4 min, i.e. 2.5%) when phenol read indicator was used and 48 sec (17.9±0.8 min, i.e. 4.5%) when HNB was applied (Fig. S3a). This is a small variation taking into consideration that the reactions were different preparations and not from a single master mix. Regarding the reaction-speed, the difference between qcLAMP and real-time fluorescent LAMP detection was found to be around 5.5 min (Fig. S3b); this difference is even smaller (by approximately 2 min) if we consider the fact that real-time fluorescent LAMP measurements start only after the heat block has reached the required temperature (63ºC) while in the qcLAMP device heating starts at t=0 min when the heater is still at room temperature. Finally, the efficiency and sensitivity of qcLAMP inside a complex (saliva) sample was demonstrated during the detection of down to 400 CFU/ml (2 copies in the reaction) (Fig. S4). The use of 5 μl of crude saliva in a 25 μl LAMP reaction translates to an impressive final crude sample concentration of 20% in contrast to the commonly required 10% or less.

Overall, the device showed excellent stability and reproducibility during the continuous and undisturbed operation of a testing period of over 12 months; using a 10000 mAh power-bank, the device was able to run non-stop for approximately 5 h (Fig. S5).

qcLAMP testing for SARS-CoV-2. To validate the qcLAMP for infectious disease testing, we focused on the recent COVID-19 pandemic and urgent need for SARS-CoV-2 detection. Initially, the capability of qcLAMP to provide quantitative results was tested by deriving a calibration curve from a wide range of starting template material. For this curve, DNA derived from Influenza A was used as a reference molecule within the range of 10^1 to 10^9 copies. Figure 3a shows a calibration curve produced by triplicate measurements for Influenza A detection (Fig. S6a). The highest template concentration showed a time-to-positive result at 11.8±0.2 min while the lowest at 20.0±2.4 min. The achieved detection limit was 10 copies per reaction or 0.4 copies per μl input. The reproducibility of our device in respect to the same initial target concentration (10^9 copies/reaction) was evaluated by monitoring 21 positive and 7 negative LAMP reactions. The standard deviation for the average time-to-positive results was only 36 sec (Fig. S6b); no increase in the color index units was detected with the negative reactions (Fig. S6c).

Following the above calibration, we evaluated the performance of the device for the detection of SARS-CoV-2 during simultaneous reverse transcription and isothermal amplification targeting the N gene in clinical samples, starting from RNA extracted from patients' nasopharyngeal or oropharyngeal swabs. We initially performed a set of qcLAMP measurements with serial dilutions of extracted total RNA from a SARS-CoV-2 positive sample with a reported Ct value of 19 (Fig. 3b). The real-time colorimetric curves were used to correlate the time-to-positive results with the viral RNA concentrations (Fig. 3c). A very good correlation was observed (R=0.99) which verified the ability to extract quantitative information using the

bioRxiv preprint doi: https://doi.org/10.1101/2020.07.22.215251; this version posted July 24, 2020. The copyright holder for this preprint (which was not certified by peer review) is the author/funder. All rights reserved. No reuse allowed without permission.

newly developed method. Furthermore, by employing a commercially available kit we have managed to detect 5 copies of viral RNA per LAMP reaction within approximately 20 min (Fig. S6d).

Additionally, 89 patient samples consisting of 38 qRT-PCR positive and 51 negative for SARS-CoV-2 samples were tested with the qcLAMP method. The positive samples had reported qRT-PCR Ct values ranging from 16 to 36.8. The fastest observed time-to-positive result with qcLAMP was 12.5 min for a sample with a Ct value of 16 while the maximum was 23 min for a Ct of 36.7. Thirty-seven (37/38) of the positive samples (with respect to qRT-PCR) were successfully identified with qcLAMP in the first attempt. Only one (1/38) was identified as positive after a second repeat on a second run. The correlation of qRT-PCR Ct values and time-to-positive results with qcLAMP is shown in Fig. 3d. It should be noted that these were independent runs performed in different days within 3 weeks. In parallel to N- gene testing, detection of the human RNA target (RNase P) was carried out as a positive control.

Forty-seven (47/51) negative samples for SARS-CoV-2, 6 of which had been found positive for other viruses (Influenza, CMV, RSV, Adenovirus, and Enterovirus) were successfully identified as negative without any indication of cross-reactivity. Furthermore, we found that 4 (4/51) of the stored samples previously identified as SARS-CoV-2 positive were negative with our device. Running a second qRT-PCR verified our results; this observation was attributed to poor RNA quality after freezing and thawing. Finally, among the 89 samples used, 12 (both positive and negative) were blindly tested and successfully identified with our method. The results from this study have important implications in the context of developing reliable molecular diagnostic tools, given the demonstrated excellent performance of the qcLAMP methodology with 0% of false positive and only 2.6% false negative results (Fig. 3e).

bioRxiv preprint doi: https://doi.org/10.1101/2020.07.22.215251; this version posted July 24, 2020. The copyright holder for this preprint (which was not certified by peer review) is the author/funder. All rights reserved. No reuse allowed without permission.

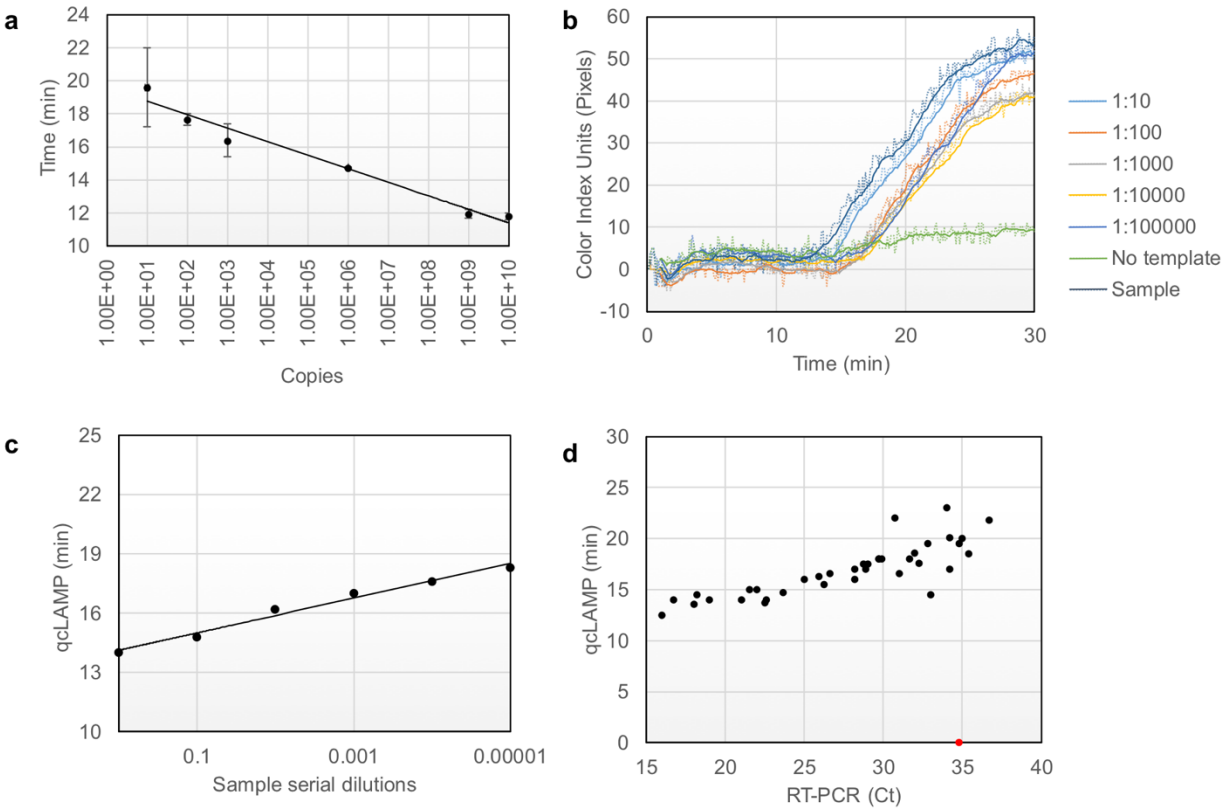

e

Samples	Measured	Identified	Accuracy	False P.	False N.
Total	89	88	98.88%		
Negative	51	51	100.00%	0.00%	
Infected	38	37	97.37%		2.63%

Figure 3: (a) Calibration curve using Influenza A DNA template ranging from 10^1 to 10^9 copies per reaction. (b) Serial dilutions of a SARS-COV-2 positive sample with a reported Ct value of 19 were measured with the qcLAMP method. (c) Correlation (R=0.99) between the qcLAMP time-to-positive results and the viral RNA concentration based on a 10-fold serial dilutions. (d) Scatter plot of the Ct values for 38 positive samples (ranging from 16 to ~37) versus the qcLAMP time-to-positive (ranging from 12.5 to 23 min). qcLAMP measurements were performed in different days within 3 weeks using stored (-80ºC) RNA samples. Only one point (red) was missed by qCLAMP in the first run. (e) Performance evaluation of SARS-CoV-2 qcLAMP assay with 89 clinical samples including 38 COVID-19 positive and 51 negative.

Quantitative detection of *BRAF* V600E mutation from FFPE tissues and clinical validation. In a second attempt, we employed our system to detect various ratios of the *BRAF* V600E mutation in the presence of wild type (wt) alleles, a test of significance to companion diagnostics. Isolated genomic DNA (from patient samples) containing the mutation of interest (mut) was mixed with wild type DNA (wt) to a total amount of 100 ng DNA in the following (mut:wt) ratios: 50%-10%-5%-1%-0.1%-0.01%-0%. The lowest ratio (0.01%), corresponding to the limit of detection, contained 10 pg of mutant DNA or approximately 2-3 mutant copies[47].

bioRxiv preprint doi: https://doi.org/10.1101/2020.07.22.215251; this version posted July 24, 2020. The copyright holder for this preprint (which was not certified by peer review) is the author/funder. All rights reserved. No reuse allowed without permission.

Triplicate LAMP reactions were measured, in random order, in the phenol red channel for 45 min in total. All different ratios showed a positive response within the first 30 min while for the 0% (or 100 ng wt) no signal change was observed. Figure 4a illustrates a set of real-time colorimetric curves for the whole range of measured ratios. The average time response for each ratio showed excellent correlation (R=0.995) with the starting template concentration of mutant DNA (Fig. 4b). Overall, Fig. 4b demonstrates the ability of the method to provide positive results in a wide dynamic range of more than four orders of magnitude (10 pg to 50 ng of mutant genomic DNA) and with zero background signal when only wild type DNA is used. The requirement of 100 ng genomic DNA per reaction is an amount readily obtained from one 5-μm tissue section and similar to what other methods require[48, 49].

Moreover, we investigated the possibility of performing direct detection of the *BRAF* V600E mutation from FFPE tissue without DNA extraction. Slices of paraffin tissue (1 mm) with mut:wt ratio of 50, 20, 10 and 0% were immersed in sterile water and incubated at 92ºC for 60 min; 7.5-10 μl of the solution were then transferred into LAMP reactions containing the phenol red indicator and placed in the 3D-device for another 60 min. As expected, the wt tissue sample did not show any signal change. The 50% tissue samples were found positive in approximately 30 min while the 20 and 10% after 35 and 45 min, respectively (Fig. 4c). Mixing wt and 10% preparations to a final ratio of 1% mut:wt was also found positive at 45.5 min on average but the result was reproduced only in 2 out of the 8 attempts. Figure 4d illustrates a set of real-time colorimetric curves for the 5 different ratios of mut:wt tissue samples (50-20-10-1-0%).

The detection of the mutation in the 1% ratio was not always possible for two main reasons. Firstly, the LAMP reaction contained a fraction (10 μl) of a DNA preparation (1/2 of a 15-μm tissue slice melted in 100 μl water) that was not expected to contain more than 20 ng of genomic DNA. Secondly, the DNA preparation through melting was of low purity compared to standard DNA extraction methods that utilize protein digestion and overnight lysis steps[50, 51]. Larger slices of tissue, not available in the current study, could improve the reproducibility for the 1% ratio. The melting process could also be improved by using a combination of a commercially available lysis solution with a DNA intercalating colorimetric dye (e.g. crystal violet). In this study, melting in water was employed not only as a simple and cost-effective solution but also for compatibility issues with the pH dependent phenol red color indicator.

Finally, the presence of the *BRAF* V600E mutation in genomic DNA extracted from 12 clinical biopsy samples from cancer patients was investigated in blind tests with our device. A sample of 100 ng of extracted genomic DNA were tested in the phenol red channel while the same DNA preparation was used for Sanger sequencing and the ddPCR method. The presence of the mutation was verified by an increase in the color index units in five out of the 12 tested samples while the rest showed no change in pixels (Fig. 4e). Four of the positive samples were identified in less than 30 and one in less than 40 min. These results were in total agreement with Sanger sequencing method and the droplet digital PCR (ddPCR). According to ddPCR, the concentration of mutant copies successfully identified by the device ranged from 12.1 to 173 copies/μl (Fig. 4f).

bioRxiv preprint doi: https://doi.org/10.1101/2020.07.22.215251; this version posted July 24, 2020. The copyright holder for this preprint (which was not certified by peer review) is the author/funder. All rights reserved. No reuse allowed without permission.

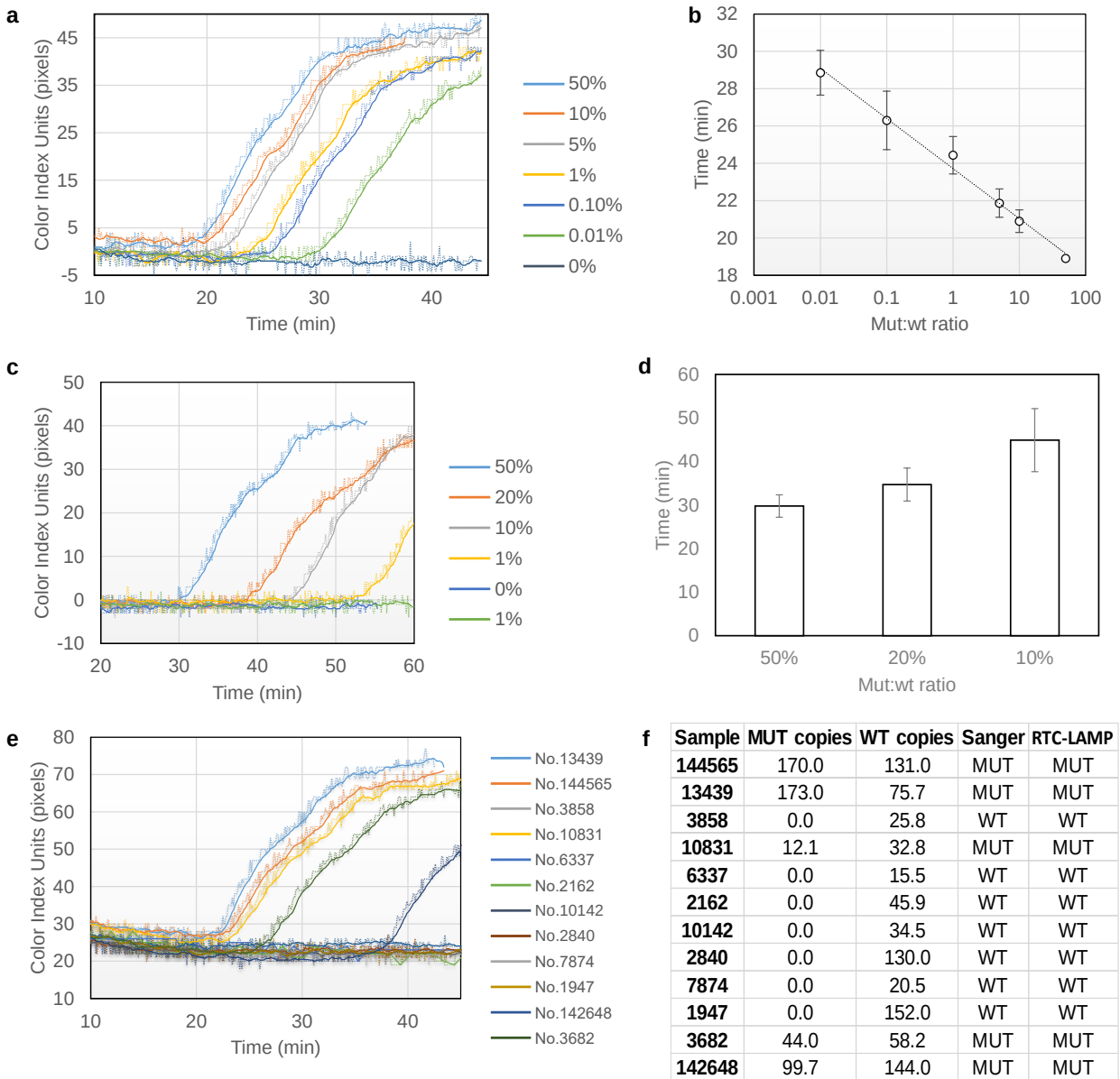

f

Sample	MUT copies	WT copies	Sanger	RTC-LAMP
144565	170.0	131.0	MUT	MUT
13439	173.0	75.7	MUT	MUT
3858	0.0	25.8	WT	WT
10831	12.1	32.8	MUT	MUT
6337	0.0	15.5	WT	WT
2162	0.0	45.9	WT	WT
10142	0.0	34.5	WT	WT
2840	0.0	130.0	WT	WT
7874	0.0	20.5	WT	WT
1947	0.0	152.0	WT	WT
3682	44.0	58.2	MUT	MUT
142648	99.7	144.0	MUT	MUT

Figure 4: (a) Real-time colorimetric curves corresponding to mut:wt starting template ratios spanning more than four orders of magnitude. (b) Calibration curve produced from real-time data of triplicate colorimetric LAMP measurements; $y = -1.165\ln(x) + 23.72$ ($R^2 = 0.9902$). (c) Real-time data corresponding to tissue samples of various mut:wt ratios. The 1% was not consistently produced (yellow vs green line). (d) Comparison of real-time data for 10, 20 and 50% mut:wt tissue samples measured directly in the qcLAMPdevice without DNA purification. (e) Real time colorimetric LAMP results of 12 patient samples analyzed with the qcLAMP 3D device (blind tests). (f) Comparison of ddPCR, Sanger and qcLAMP test results of 12 clinical samples. The ddPCR method provided additional information regarding the concentration of mutant and wild type copies per analyzed sample.

Discussion

Low-cost portable and quantitative nucleic acid detection is desirable for molecular diagnostics at the POC. Colorimetric LAMP, one of the simplest and most suitable formats for POC applications is based solely on end-point measurements and derives primarily qualitative results. Here we describe a device that offers for the first time the ability to perform real-time

bioRxiv preprint doi: https://doi.org/10.1101/2020.07.22.215251; this version posted July 24, 2020. The copyright holder for this preprint (which was not certified by peer review) is the author/funder. All rights reserved. No reuse allowed without permission.

colorimetric LAMP and extract quantitative information in a similar manner to real-time fluorescent nucleic acid amplification methods but without their associated complexity and high cost. The newly developed device is based on a contamination-free closed tube format obviating the need for microfluidic chips, peristaltic pumps, fluorescent detectors and multiple step protocols employed elsewhere[13, 26, 39, 40, 52]. It can achieve a similar limit of detection to the real-time fluorescent PCR and LAMP protocols (1-10 copies/reaction) while it does not suffer from background non-specific signal or need for signal drift correction or precise selection of threshold values required in other more sophisticated systems[27, 28]. It displays similar time-to-result with real-time fluorescent LAMP (Fig. S3); in addition, it can be performed in the presence of crude samples, such as 20% saliva (Fig. S4) or tissue-specimens without prior nucleic acids extraction (Fig 4c).

The clinical utility of the new technology and broad applicability are demonstrated in two applications. First, during the development of an assay for SARS-CoV-2 RNA detection and validation using COVID19 patients' samples and against the standard qRT-PCR method recommended by the WHO and the CDC. The targeted N gene, selected for the proof-of-concept, was shown to be specific for SARS-CoV-2 since samples positive for respiratory or other viruses exhibited no cross-reactivity. Compared to qRT-PCR, the qcLAMP method delivers results within 23 min demonstrating at the same time a very good sensitivity and specificity (Table 1). Our results complement current efforts[38, 53-55] by the scientific community to provide a reliable solution for SARS-CoV-2 testing with desirable characteristics the fast analysis time, no need for complex infrastructure and access to commercially available off-the shelf reagents. To our knowledge, the 97.4% sensitivity and 100% specificity demonstrated with the qcLAMP using extracted RNA from patients' samples is one of the best reported so far.

The qcLAMP methodology was also applied as a companion diagnostic tool for *BRAF* V600E mutation detection. The demonstrated ability to detect as low as 2-3 mutant copies within an abundance of wild-type background alleles (0.01% ratio) was more than two orders of magnitude better than commonly employed methods (Table 1). Among them are the Sanger sequencing which is the clinical standard, pyrosequencing, the Cobas test and the Infinity assay, all of which have a reported LOD of ≥5%[48, 56, 57]. Only the ddPCR has a better reported LOD of 0.001%[49]; however, ddPCR is expensive and unsuitable for companion diagnostics. Moreover, all 12 clinical samples tested blindly were identified according to Sanger sequencing and ddPCR. The current application of the qcLAMP methodology can provide a valuable tool for POC pharmacogenetic tests at the time treatment is required, alleviating delays associated with testing in centralized labs[58]. Such examples include the prescription of vemurafenib to melanoma patients carrying the *BRAF* V600E, or warfarin and clopidogrel (Plavix) drugs prescribed for cardiovascular diseases-treatment, the response of which is affected by genetic polymorphisms (*VKORC1*, *CYP2C9* and *CYP2C19* genes).

Despite of the final application, a considerable advantage of our methodology is the simple yet robust instrumentation employed, allowing fast prototyping through 3D-printing at a record time of <12 h; rapid scaling up of the production is foreseen due to the low complexity of the design. Regarding cost, it is anticipated to fall well below that of a water bath typically used for heating the samples in colorimetric LAMP applications at resource-limited areas. Moreover, the device is lightweight, portable, can be battery-operated and is fully controlled by a smartphone. It, thus, falls well within on-going efforts to develop smartphone based POC

bioRxiv preprint doi: https://doi.org/10.1101/2020.07.22.215251; this version posted July 24, 2020. The copyright holder for this preprint (which was not certified by peer review) is the author/funder. All rights reserved. No reuse allowed without permission.

devices for large-scale rapid testing combined with spatiotemporal surveillance and data transfer through the cloud[59]. The above characteristics make the qcLAMP device a particularly attractive solution for global diagnostics, with the potential of manufacturing and production to take place directly in the low- or middle-income countries.

Method	qcLAMP	qRT-PCR	Sanger	ddPCR
TECHNOLOGY - ENGINEERING				
Instrumentation	3D printed device	Benchtop equipment	Benchtop equipment	Benchtop equipment
Manufacturability	Lab-based production in 12h	Commercial (Optical filters)	Commercial (Optical filters)	Commercial (Optical filters)
Cost	Low	High	High	Very High
Complexity	Low	High	High	Very High
Portability	Lightweight, battery operated	No	No	No
Connectivity	Smartphone/ cloud connection	PC based	PC based	PC based
Multiple samples	Yes (<10)	Yes (high throughput)	Yes (high throughput)	Yes (high throughput)
Quantitative	Yes	Yes	No	Yes

Method	**qcLAMP**	**qRT-PCR**	**qcLAMP**	**Sanger**	**ddPCR**
	SARS-CoV-2 ASSAY		**BRAF V600E ASSAY**		
Detection steps	1	2	1	2	2
Temperature	65ºC	50ºC (RT) (95ºC – 55ºC)x45 cycles	65ºC	multiple	multiple
Assay time	30 min	80 min	N/A	N/A	N/A
Sample-to-result time	45 min	2 h 30 min	<2h	>24h	>2h
Target/control	N gene/ RNase P	RdRp gene/ RNase P	*BRAF* V600E/WT	BRAF V600E/WT	BRAF V600E/WT
Preparatory steps	NA extraction	NA extraction	1 (DNA extraction or tissue heating)	2 (DNA extraction & thermal cycling)	2 (DNA extraction & droplets generation)
Analytical performance	5 copies/ reaction	Not available	0.01% (mut:wt ratio)	5% (mut:wt ratio)	0.001% (mut:wt ratio)

Table 1: Comparison of the qcLAMP, qRT-PCR P, Sanger sequencing and ddPCR methods for the two applications.

The reported device can serve as an open platform for colorimetric LAMP assays, for applications and beyond healthcare. The system could be used for the detection of food-borne pathogens at production lines with limited analytical capabilities or at on-site inspections where fast results are necessary. Plant-borne pathogens detection in the field combined with on-line surveillance will allow better control of the use of pesticides and other chemicals leading to safer products and increased crop-yields. Future work in our group explores the capabilities and full potential of qcLAMP in the above areas; we would like to invite scientists to implement as well this promising new tool in their research both in the lab for performing routine LAMP assays and in any relevant application in the field.

bioRxiv preprint doi: https://doi.org/10.1101/2020.07.22.215251; this version posted July 24, 2020. The copyright holder for this preprint (which was not certified by peer review) is the author/funder. All rights reserved. No reuse allowed without permission.

Methods

qcLAMP device design and construction. The qcLAMP device consists of five individual parts: The main body (hosting all the electronic parts), the heating element holder, the vial holder, the bottom and top cover. All parts were made from polylactic acid (PLA) purchased from Polymaker (Netherlands) or 3DPrima (Sweden), except for the heating element holder which was made from high Tg co-polyester (HT) purchased from Colorfabb (Netherlands). HT is known for having a high glass transient temperature (~ 100° C), thus making it a suitable material for use in hot environments. All parts were designed by using openSCAD software. The PLA parts were 3D-printed in the Bolt pro 3D printer from Leapfrog (Netherlands), while the HT parts in the TAZ6 3D printer from Lulzbot (U.S.A.). The vial holder was designed to fasten magnetically on the top cover; the latter is also connected to the main body *via* magnets. The PCB board is fixed firmly on the heating element holder, which also connects tightly to the main body. The bottom part/cover of the device encloses and protects the electronic components. The only freely moving parts of the system are the top cover and vial holder. The manufacturing protocol produces two boxes in almost 16 hours (standard speed, 0.25mm layer thickness) or 10 hours (high speed, 0.38mm layer thickness) due to the independent dual extruders that the Bolt pro offer. This way, two boxes are manufactured in parallel. The fabrication and assembly of the system can be completed within half a day.

Electronics design and smartphone app development. The electronics layer of the qcLAMP device consists of three main components: a Raspberry Pi Zero W board (RPi), a Camera Pi module and a custom made PCB RPi Hat. The RPi operates as a central microcomputer while the Camera Pi is used for image acquisition. The PCB Hat (designed with KiCAD software) is used as an interface dedicated to control the power supply and the operation of heater, sensor and LEDs (Fig. S7). The Software layer of the device can be further divided into two categories: the software running on the RPi and the software deployed as an Android application on a mobile device. A full systems' architecture is depicted in Fig. S8. A user-friendly interface (Android application) is used to set the temperature, colorimetric dye and an interval for the image acquisition. These initial settings are transmitted via a bluetooth low energy (BLE) connection to the corresponding bluetooth peripheral module, running inside the RPi. After setting the parameters of the experiment, a python module at the RPi end initiates the image acquisition and analysis. Each image is sent to a second python module which undertakes the image analysis procedure. The first step of this python module is to define a rectangle area on the image of the reaction tubes (Fig. S9) and continue with the application of the colorimetric analysis as described in Digital image analysis section.

Device performance evaluation. Evaluation experiments were performed with an attenuated strain of *Salmonella enterica* serovar Typhimirium. *Salmonella* was grown overnight in Luria−Bertani (LB) medium; cultures were subsequently measured spectrophotometrically (OD600) and adjusted at OD600:1 corresponding to a cell concentration of 1−1.5 × 10^9 CFU/mL. Serial dilution of the above cells suspension by LB was carried out to reach the required concentration. The *Salmonella* invasion gene invA was targeted by a set of six primers (Metabion, Germany), two outer (F3 and B3), two inner (FIP and BIP) and two loop (Loop-F and Loop-B). The sequences of the primers (5'-3') were as follows:
FIP:GACGACTGGTACTGATCGATAGTTTTTCAACGTTTCCTGCGG,
BIP:CCGGTGAAATTATCGCCACACAAAACCCACCGCCAGG,
F3:GGCGATATTGGTGTTTATGGGG,
B3:AACGATAAACTGGACCACGG,
Loop F:GACGAAAGAGCGTGGTAATTAAC,
Loop B:GGGCAATTCGTTATTGGCGATAG.
The LAMP reagent mix in a total volume of 25 μL contained 12.5 μL of WarmStart or Colorimetric WarmStart 2 × Master Mix (New England BioLabs) or Bsm polymerase (Thermo Scientific), 1.8 μM FIP

bioRxiv preprint doi: https://doi.org/10.1101/2020.07.22.215251; this version posted July 24, 2020. The copyright holder for this preprint (which was not certified by peer review) is the author/funder. All rights reserved. No reuse allowed without permission.

and BIP, 0.1 μM F3 and B3, 0.4 μM Loop-F and Loop-B, and 2.5 μL of sterile water or any crude sample mixed with 1 μL of cells. The HNB color indicator was added to a final concentration of 160μM when used. LAMP was performed in the qcLAMP device at 63°C. After amplification, the products were analyzed using electrophoresis on a 2% agarose gel containing GelRed (Biotium) and visualized under UV light.

qcLAMP testing for SARS-CoV-2. For the calibration curve, saliva from healthy donors was purchased from Lee Biosolutions, USA. A volume of 2-5μl or saliva was mixed with 1μL of *Salmonella* cells followed by cell lysis at 95 °C for 5 min, mixing with the LAMP cocktail (described in the previous section) and placing it in the device at 63°C. The primers used for Influenza A detection, purchased by Metabion (Germany) were as follows:
F3: AACAGTAACACACTCTGTCA, B3: CATTGTCTGAATTAGATGTTTCC,
FIP: CCAAATGCAATGGGGCTACCATCTTCTGGAAGACAAGCA,
BIP: TAACATTGCTGGCTGGATCCTACAATGTAGGACCATGATCT, LF:
CCTCTTAGTTTGCATAGTTTTCCGT,
LB: CCAGAGTGTGAATCACTCTCCAC.
The DNA template used for the Influenza measurements was a PCR product of 452bp corresponding to the HA gene of Influenza A.
For SARS-CoV-2 detection, the primers used were targeting the N gene, described elsewhere[53], were as follows:
F3: AACACAAGCTTTCGGCAG,
B3:GAAATTTGGATCTTTGTCATCC,FIP:TGCGGCCAATGTTTGTAATCAGCCAAGGAAATTTTGGGGA
C,
BIP: CGCATTGGCATGGAAGTCACTTTGATGGCACCTGTGTAG,
LF: TTCCTTGTCTGATTAGTTC,
LB: ACCTTCGGGAACGTGGTT.
2 μl of total RNA extracted from patient samples was used for RTC-LAMP. All experiments for the calibration curve with Influenza and SARS-CoV-2 were performed with the Colorimetric LAMP mix from NEB. Real-time colorimetric LAMP (qcLAMP) was performed with our device for 30 min per run. Tests were performed using 2μl of extracted total RNA from patient samples stored at –80ºC. qcLAMP was targeting a viral RNA corresponding to the N gene of the SARS-CoV-2 genome. A second RNA target (ORF1a) was also available but selectively tested (data not shown). A human RNA target (RNase P) was used as a positive reference with a previously described set of primers[53]. No-template reactions were periodically performed for checking the quality of the reagents (e.g. contamination) and the temperature stability of the device. Synthetic SARS-CoV-2 RNA was purchased from BIORAD (SARS-CoV-2 Standard #COV019 and SARS-CoV-2 Negative #COV000).

Sample collection. Nasopharyngeal or oropharyngeal swabs were acquired from patients with suspicion of COVID-19 infection. Clinical swab samples were collected in VTM from several public and private hospitals of Greece and forwarded to the National SARS-CoV-2 Reference Laboratory, Hellenic Pasteur Institute for further testing.

qRT-PCR assays for SARS-CoV-2. Viral RNA was extracted from 200μl of clinical samples using the NucliSens easyMAG automated system (BioMérieux, Marcy l'Etoile, France). A 106bp fragment of the SARS-CoV-2 virus RdRp gene was amplified according to an in-house qPCR protocol proposed by the WHO and the National Reference Center for Respiratory Viruses, Institut Pasteur, Paris. As a confirmatory assay, the E gene assay from the Charité protocol was used[60] by real-time RT-PCR.

bioRxiv preprint doi: https://doi.org/10.1101/2020.07.22.215251; this version posted July 24, 2020. The copyright holder for this preprint (which was not certified by peer review) is the author/funder. All rights reserved. No reuse allowed without permission.

SeraCare's SARS-CoV-2 AccuPlex solution 5000copies/ml (Material number 0505-0126) was used for limit-of detection testing. 1 μL of the solution was directly placed in the LAMP mix or after 10 min of heating at 80ºC.

Detection of *BRAF* V600E mutation from extracted genomic DNA. Loop-mediated amplification was conducted by using genomic DNA, BRAF V600E Reference Standard and BRAF Wild Type Reference Standard, purchased from Horizon Discovery or extracted from formalin-fixed and paraffin-embedded (FFPE) tissue (clinical samples). A set of six primers (Metabion, Germany) were used for the detection of BRAF V600E mutation; two outer (F3 and B3), two inner (FIP and BIP) and two loop (Loop-F and Loop-B). The sequences of the primers (5'-3') were as follows: FIP:TCTGTAGCTAGCAGATATATTTCTTCATGAAGACCT, BIP: AGAAATCTCGATTCCACAAAATGGATCCAGA, F3: GGAAAATGAGATCTACTG, B3: TCTCAGGGCCAA, LF: ACCAAAATCACCTATTT, LB: GGAGTGGGTCCC. LAMP was carried out in a total of 25μl reaction mixture containing 1.6μM of the forward inner primer (FIP), 1.6μM of the backward inner primer (BIP), 0.2μM of the forward outer primer (F3), 0.2μM of the backward inner primer (B3) and for the loop primers 0.8μM of loop-forward (LF) and 0.8μM of loop-backward (LB) as described previously[29]. The total concentration of genomic DNA used was 100ng/μl, which contained wild-type and/or mutant DNA, adjusted depending on the number of mutant copies to be detected (50%-0.01% mutant DNA). Positive and negative controls were included in each set of reactions and every precaution needed in order to avoid cross-contamination. 2 μl of genomic DNA were mixed with LAMP primers, denatured for 5 min at 92ºC and quickly placed on ice. The solution was subsequently mixed with 12.5 μL WarmStart® colorimetric LAMP and the reactions were finally placed in the qcLAMP device for real-time amplification monitoring at 63ºC.

Direct detection of *BRAF* V600E from formalin fixed paraffin tissue. Tissue slices of various mutant:wild type ratios for the BRAF V600E mutation were purchased from Horizon Discovery. Slices of 15 μm (or 1 mm in length) were immersed in 100 μl of ddH_2O and heated at 95°C for 65 min followed by a brief centrifugation step at 13000 rpm for 2 min. 10 μl of the solution were then mixed with the LAMP primers and denatured at 92ºC for 5 min. For the 1% ratio, a 100% wild type solution was mixed with a 10% to the final volume of 10 μl. After the denaturation step, each solution was placed on ice before mixing it with 12.5 μL of WarmStart® colorimetric LAMP and placing in the bioPix device for real-time amplification monitoring at 63ºC.

Formalin-fixed and paraffin-embedded (FFPE) tissue processing and DNA extraction of the clinical samples. Twelve FFPE samples from patients with cancer were investigated, including 4 melanomas, 4 colorectal cancer tissues and 4 non-small cell lung cancer samples. The research protocol was approved by the Ethics Committee of the University Hospital of Heraklionand all participants provided written informed consent. Tumor areas were micro-dissected to enrich the analyzed specimen with cancer cells and DNA was extracted using the QIAamp DNA Micro Kit (Qiagen). DNA concentration was determined spectrophotometrically by the absorbance measurement at 260nm and all samples were kept at -20oC until use.

Sanger sequencing for the clinical samples. Samples from cancer patients were tested by Sanger sequencing, which is a gold standard method for detecting DNA mutations. In more details, a PCR assay was designed to amplify *BRAF* exon 15, which includes the mutation hotspot that encodes the V600E variant. The primer sequences used in this study were as follows: *BRAF* forward 5'-TGT TTT CCT TTA CTT ACT ACA CCT CA-3' and reverse 5'- GCC TCA ATT CTT ACC ATC CA-3' (PCR amplicon of 160bp). PCR products were then electrophoresed on 2.0 % (w/v) agarose gel to check the presence of specific amplification products. Unincorporated PCR primers and dNTPs were removed from the PCR products

bioRxiv preprint doi: https://doi.org/10.1101/2020.07.22.215251; this version posted July 24, 2020. The copyright holder for this preprint (which was not certified by peer review) is the author/funder. All rights reserved. No reuse allowed without permission.

using the Nucleospin PCR clean-up kit (Macherey-Nagel) according to the manufacturer's protocol. The sequencing reactions were performed in a final volume of 10.0 µl using: 2.0 µl of purified PCR product, BigDye Terminator v3.1 Sequencing reagents (Applied Biosystems), and 125nM each of the forward and reverse primers. The products were purified using ethanol precipitation and Sanger sequencing was performed by capillary electrophoresis (ABI3130, Applied Biosystems). Sequencing analysis v5.4 software (Applied Biosystems) was used to analyze the results.

Droplet Digital PCR for *BRAF* V600E Quantification. DNA samples with the *BRAF* V600E mutation, as determined with Sanger sequencing, were by the ddPCR system for absolute quantification of mutant alleles and wild-type alleles. The ddPCR was performed using the QX200 Droplet Digital PCR System (Bio-Rad) and the ddPCR *BRAF* V600 Screening Multiplex Kit (Bio-Rad) for 3 different hot-spot codon V600 mutations (V600E, V600K, and V600R), according to the manufacturer's protocol. Each sample was tested in two technical replicates and every ddPCR run included negative template controls (NTCs) and positive controls (*BRAF* mutant homozygous and heterozygous cancer cell lines and Wild-Type (WT) samples). Samples were mixed with 70.0µL of droplet generator oil for probes (Bio-Rad) and partitioned into up to 20,000 droplets using the Bio-Rad QX-200 droplet generator (Bio-Rad). Then, 40.0µL of emulsion for each sample, was transferred to 96-well plates (Bio-Rad) and PCR was done on C1000 Touch thermal cycler (Bio-Rad), using the following conditions: 95°C for 10 min, and 40 cycles of 94°C for 30 s, 55°C for 1 min, and 98°C for 10 min. The plate was then transferred and read in the FAM and HEX channels using the QX200 droplet reader (BioRad). Data analysis was performed using the QuantaSoft Analysis Pro Software (Version 1.0.596) to assign positive/negative droplets and convert counts to target copies/µL of reaction. Threshold was manually set for each sample, based on positive control samples (mutant and WT for each channel).

Data availability

The authors declare that all data supporting the findings in this study are available within the paper and its Supplementary Information files.

References

1. Higuchi, R., Dollinger, G., Walsh, P.S. & Griffith, R. Simultaneous amplification and detection of specific DNA sequences. *Biotechnology (N Y)* **10**, 413-417 (1992).
2. Higuchi, R., Fockler, C., Dollinger, G. & Watson, R. Kinetic PCR analysis: real-time monitoring of DNA amplification reactions. *Biotechnology (N Y)* **11**, 1026-1030 (1993).
3. Heid, C.A., Stevens, J., Livak, K.J. & Williams, P.M. Real time quantitative PCR. *Genome Res* **6**, 986-994 (1996).
4. Valasek, M.A. & Repa, J.J. The power of real-time PCR. *Adv Physiol Educ* **29**, 151-159 (2005).
5. Furlan, I., Domljanovic, I., Uhd, J. & Astakhova, K. Improving the Design of Synthetic Oligonucleotide Probes by Fluorescence Melting Assay. *Chembiochem* **20**, 587-594 (2019).
6. Gudnason, H., Dufva, M., Bang, D.D. & Wolff, A. Comparison of multiple DNA dyes for real-time PCR: effects of dye concentration and sequence composition on DNA amplification and melting temperature. *Nucleic Acids Res* **35** (2007).
7. Becherer, L. et al. Loop-mediated isothermal amplification (LAMP) - review and classification of methods for sequence-specific detection. *Anal Methods-Uk* **12**, 717-746 (2020).
8. Nagamine, K., Hase, T. & Notomi, T. Accelerated reaction by loop-mediated isothermal amplification using loop primers. *Mol Cell Probe* **16**, 223-229 (2002).
9. Notomi, T. et al. Loop-mediated isothermal amplification of DNA. *Nucleic Acids Res* **28** (2000).

bioRxiv preprint doi: https://doi.org/10.1101/2020.07.22.215251; this version posted July 24, 2020. The copyright holder for this preprint (which was not certified by peer review) is the author/funder. All rights reserved. No reuse allowed without permission.

10. Baikunje, N. et al. Comparative evaluation of loop-mediated isothermal amplification (LAMP) assay, GeneXpert MTB/Rif and multiplex PCR for the diagnosis of tubercular lymphadenitis in HIV-infected patients of North India. *Mol Cell Probes* **48**, 101459 (2019).
11. Khan, M. et al. Comparative Evaluation of the LAMP Assay and PCR-Based Assays for the Rapid Detection of Alternaria solani. *Front Microbiol* **9**, 2089 (2018).
12. Francois, P. et al. Robustness of a loop-mediated isothermal amplification reaction for diagnostic applications. *Fems Immunol Med Mic* **62**, 41-48 (2011).
13. Papadakis, G. et al. 3D-printed Point-of-Care Platform for Genetic Testing of Infectious Diseases Directly in Human Samples Using Acoustic Sensors and a Smartphone. *ACS Sens* **4**, 1329-1336 (2019).
14. Snodgrass, R. et al. A portable device for nucleic acid quantification powered by sunlight, a flame or electricity. *Nat Biomed Eng* **2**, 657-665 (2018).
15. Mori, Y., Kitao, M., Tomita, N. & Notomi, T. Real-time turbidimetry of LAMP reaction for quantifying template DNA. *J Biochem Bioph Meth* **59**, 145-157 (2004).
16. Nixon, G.J. et al. A novel approach for evaluating the performance of real time quantitative loop-mediated isothermal amplification-based methods. *Biomol Detect Quantif* **2**, 4-10 (2014).
17. Calmy, A. et al. HIV viral load monitoring in resource-limited regions: Optional or necessary? *Clin Infect Dis* **44**, 128-134 (2007).
18. Takano, C. et al. Development of a Novel Loop-Mediated Isothermal Amplification Method to Detect Guiana Extended-Spectrum (GES) beta-Lactamase Genes in Pseudomonas aeruginosa. *Frontiers in Microbiology* **10** (2019).
19. Chen, S.Y. & Ge, B.L. Development of a toxR-based loop-mediated isothermal amplification assay for detecting Vibrio parahaemolyticus. *Bmc Microbiol* **10** (2010).
20. Giuffrida, M.C. & Spoto, G. Integration of isothermal amplification methods in microfluidic devices: Recent advances. *Biosens Bioelectron* **90**, 174-186 (2017).
21. Ma, Y.D., Chen, Y.S. & Lee, G.B. An integrated self-driven microfluidic device for rapid detection of the influenza A (H1N1) virus by reverse transcription loop-mediated isothermal amplification. *Sensor Actuat B-Chem* **296** (2019).
22. Chuang, T.L., Wei, S.C., Lee, S.Y. & Lin, C.W. A polycarbonate based surface plasmon resonance sensing cartridge for high sensitivity HBV loop-mediated isothermal amplification. *Biosens Bioelectron* **32**, 89-95 (2012).
23. Safavieh, M., Ahmed, M.U., Tolba, M. & Zourob, M. Microfluidic electrochemical assay for rapid detection and quantification of Escherichia coli. *Biosens Bioelectron* **31**, 523-528 (2012).
24. Stedtfeld, R.D. et al. Gene-Z: a device for point of care genetic testing using a smartphone. *Lab Chip* **12**, 1454-1462 (2012).
25. Liao, S.C. et al. Smart cup: A minimally-instrumented, smartphone-based point-of-care molecular diagnostic device. *Sensor Actuat B-Chem* **229**, 232-238 (2016).
26. Zhang, X.Z., Lowe, S.B. & Gooding, J.J. Brief review of monitoring methods for loop-mediated isothermal amplification (LAMP). *Biosens Bioelectron* **61**, 491-499 (2014).
27. Papadakis, G. et al. Micro-nano-bio acoustic system for the detection of foodborne pathogens in real samples. *Biosens Bioelectron* **111**, 52-58 (2018).
28. Hajian, R. et al. Detection of unamplified target genes via CRISPR-Cas9 immobilized on a graphene field-effect transistor. *Nature Biomedical Engineering* **3**, 427-437 (2019).
29. Toumazou, C. et al. Simultaneous DNA amplification and detection using a pH-sensing semiconductor system. *Nat Methods* **10**, 641-646 (2013).
30. Quyen, T.L., Ngo, T.A., Bang, D.D., Madsen, M. & Wolff, A. Classification of Multiple DNA Dyes Based on Inhibition Effects on Real-Time Loop-Mediated Isothermal Amplification (LAMP): Prospect for Point of Care Setting. *Front Microbiol* **10**, 2234 (2019).

bioRxiv preprint doi: https://doi.org/10.1101/2020.07.22.215251; this version posted July 24, 2020. The copyright holder for this preprint (which was not certified by peer review) is the author/funder. All rights reserved. No reuse allowed without permission.

31. Safavieh, M. et al. Emerging Loop-Mediated Isothermal Amplification-Based Microchip and Microdevice Technologies for Nucleic Acid Detection. *Acs Biomater Sci Eng* **2**, 278-294 (2016).
32. Sayad, A. et al. A microdevice for rapid, monoplex and colorimetric detection of foodborne pathogens using a centrifugal microfluidic platform. *Biosens Bioelectron* **100**, 96-104 (2018).
33. Song, J.Z. et al. Instrument-Free Point-of-Care Molecular Detection of Zika Virus. *Anal Chem* **88**, 7289-7294 (2016).
34. Lee, S. et al. Rapid and in-situ detection of fecal indicator bacteria in water using simple DNA extraction and portable loop-mediated isothermal amplification (LAMP) PCR methods. *Water Res* **160**, 371-379 (2019).
35. Velders, A.H., Schoen, C. & Saggiomo, V. Loop-mediated isothermal amplification (LAMP) shield for Arduino DNA detection. *BMC Res Notes* **11**, 93 (2018).
36. Kaygusuz, D., Vural, S., Aytekin, A.O., Lucas, S.J. & Elitas, M. DaimonDNA: A portable, low-cost loop-mediated isothermal amplification platform for naked-eye detection of genetically modified organisms in resource-limited settings. *Biosens Bioelectron* **141** (2019).
37. Poole, C.B. et al. Colorimetric tests for diagnosis of filarial infection and vector surveillance using non-instrumented nucleic acid loop-mediated isothermal amplification (NINA-LAMP). *Plos One* **12** (2017).
38. al, K.M.J.e. Scalable, rapid and highly sensitive isothermal detection of SARS-CoV-2 for laboratory and home testing. *bioRxiv* (2020).
39. Rodriguez-Manzano, J. et al. Reading Out Single-Molecule Digital RNA and DNA Isothermal Amplification in Nanoliter Volumes with Unmodified Camera Phones. *Acs Nano* **10**, 3102-3113 (2016).
40. Zhu, K. et al. Bio-inspired photonic crystals for naked eye quantification of nucleic acids. *Analyst* **144**, 5413-5419 (2019).
41. Tanner, N.A., Zhang, Y.H. & Evans, T.C. Visual detection of isothermal nucleic acid amplification using pH-sensitive dyes. *Biotechniques* **58**, 59-68 (2015).
42. Goto, M., Honda, E., Ogura, A., Nomoto, A. & Hanaki, K.I. Colorimetric detection of loop-mediated isothermal amplification reaction by using hydroxy naphthol blue. *Biotechniques* **46**, 167-+ (2009).
43. Miyamoto, S., Sano, S., Takahashi, K. & Jikihara, T. Method for colorimetric detection of double-stranded nucleic acid using leuco triphenylmethane dyes. *Anal Biochem* **473**, 28-33 (2015).
44. Yetisen, A.K., Martinez-Hurtado, J.L., Garcia-Melendrez, A., Vasconcellos, F.D. & Lowe, C.R. A smartphone algorithm with inter-phone repeatability for the analysis of colorimetric tests. *Sensor Actuat B-Chem* **196**, 156-160 (2014).
45. Selck, D.A., Karymov, M.A., Sun, B. & Ismagilov, R.F. Increased Robustness of Single-Molecule Counting with Microfluidics, Digital Isothermal Amplification, and a Mobile Phone versus Real-Time Kinetic Measurements. *Anal Chem* **85**, 11129-11136 (2013).
46. Damhorst, G.L. et al. Smartphone-Imaged HIV-1 Reverse-Transcription Loop-Mediated Isothermal Amplification (RT-LAMP) on a Chip from Whole Blood. *Engineering-Prc* **1**, 324-335 (2015).
47. Piovesan, A. et al. On the length, weight and GC content of the human genome. *Eur J Hum Genet* **27**, 583-583 (2019).
48. Halait, H. et al. Analytical performance of a real-time PCR-based assay for V600 mutations in the BRAF gene, used as the companion diagnostic test for the novel BRAF inhibitor vemurafenib in metastatic melanoma. *Diagn Mol Pathol* **21**, 1-8 (2012).
49. Malicherova, B. et al. Droplet digital PCR for detection of BRAF V600E mutation in formalin-fixed, paraffin-embedded melanoma tissues: a comparison with Cobas (R) 4800, Sanger sequencing, and allele-specific PCR. *Am J Transl Res* **10**, 3773-+ (2018).

bioRxiv preprint doi: https://doi.org/10.1101/2020.07.22.215251; this version posted July 24, 2020. The copyright holder for this preprint (which was not certified by peer review) is the author/funder. All rights reserved. No reuse allowed without permission.

50. Mathieson, W., Guljar, N., Sanchez, I., Sroya, M. & Thomas, G.A. Extracting DNA from FFPE Tissue Biospecimens Using User-Friendly Automated Technology: Is There an Impact on Yield or Quality? *Biopreserv Biobank* **16**, 186-190 (2018).
51. McDonough, S.J. et al. Use of FFPE-derived DNA in next generation sequencing: DNA extraction methods. *Plos One* **14** (2019).
52. Hsieh, K.W., Patterson, A.S., Ferguson, B.S., Plaxco, K.W. & Soh, H.T. Rapid, Sensitive, and Quantitative Detection of Pathogenic DNA at the Point of Care through Microfluidic Electrochemical Quantitative Loop-Mediated Isothermal Amplification. *Angew Chem Int Edit* **51**, 4896-4900 (2012).
53. Broughton, J.P. et al. CRISPR-Cas12-based detection of SARS-CoV-2. *Nat Biotechnol* (2020).
54. Park, G.S. et al. Development of Reverse Transcription Loop-Mediated Isothermal Amplification Assays Targeting Severe Acute Respiratory Syndrome Coronavirus 2. *J Mol Diagn* (2020).
55. Shan Wei, E.K., Alexandre Djandji, Stephanie Morgan, Susan Whittier, Mahesh Mansukhani, Raymond Yeh, Juan Carlos Alejaldre, Elaine Fleck, Mary D'Alton, Yousin Suh, Zev Williams Field-deployable, rapid diagnostic testing of saliva samples for SARS-CoV-2. *medRxiv* (2020).
56. Weyant, G.W., Wisotzkey, J.D., Benko, F.A. & Donaldson, K.J. BRAF mutation testing in solid tumors: a methodological comparison. *J Mol Diagn* **16**, 481-485 (2014).
57. Ihle, M.A. et al. Comparison of high resolution melting analysis, pyrosequencing, next generation sequencing and immunohistochemistry to conventional Sanger sequencing for the detection of p.V600E and non-p.V600E BRAF mutations. *BMC Cancer* **14**, 13 (2014).
58. Haga, S.B. Challenges of development and implementation of point of care pharmacogenetic testing. *Expert Rev Mol Diagn* **16**, 949-960 (2016).
59. Wood, C.S. et al. Taking connected mobile-health diagnostics of infectious diseases to the field. *Nature* **566**, 467-474 (2019).
60. Corman, V.M. et al. Detection of 2019 novel coronavirus (2019-nCoV) by real-time RT-PCR. *Eurosurveillance* **25**, 23-30 (2020).

Acknowledgements

This work has received funding from the EU through the FET-OPEN call, grant No 862840, project acronym “FREE@POC” and the Patras Science Park “Proof-of-Concept” program, Grant Agreement Number: 1718B, project acronym “Biopix”.

Author Contributions

G.P. conceived the real-time colorimetric LAMP idea and digital image analysis concept, performed the proof-of-concept and evaluation experiments, participated in the design evolution of the device and analyzed all data. A.K.P. designed, manufactured and assembled the device; assisted with the proof-of-concept evaluation, the HAT development and digital image analysis and co-designed the heaters together with N.F. N.F. developed the HAT-unit and the smartphone application and participated in the design evolution of the device. M.M and M.V. carried out all performance evaluation experiments including qcLAMP *Salmonella* detection. J.H. and E.N. prepared and provided reagents (Influenza A DNA). S.C. and V.P performed qcLAMP (Influenza, SARS-CoV-2) and qRT-PCR (SARS-CoV-2) experiments. K.G. carried out qcLAMP *BRAF* V600E detection. T.K. and A.M. supervised clinical evaluation experiments for COVID-19. S.A and K.M. performed Sanger sequencing and ddPCR experiments for *BRAF* mutation detection and analyzed the data. E.G. supervised the whole work and together with

bioRxiv preprint doi: https://doi.org/10.1101/2020.07.22.215251; this version posted July 24, 2020. The copyright holder for this preprint (which was not certified by peer review) is the author/funder. All rights reserved. No reuse allowed without permission.

G.P. wrote the manuscript. All authors read, contributed to the manuscript and agreed to its content.

Competing interests

G.P., A.K.P., N.F. and E.G. are the co-founders of BIOPIX DNA TECHNOLOGY P.C. The other authors declare no competing interests.